Desalination and Water Treatment
www.deswater.com
doi: 10.1080/19443994.2013.860629

53 (2015) 1822–1833
February

Taylor & Francis
Taylor & Francis Group

Separation efficiency and stability of thin-film composite nanofiltration membranes in long-term filtration of copper sulphate and sulphuric acid mixture

Jie Sun[a], Lin Zhang[a], Boming Xie[b], Lihang Fan[b], Sanchuan Yu[a,*]

[a]*Department of Chemistry, Zhejiang Sci-Tech University, Hangzhou 310018, China*
Tel. +86 571 86843217; Fax: +86 571 86843217; email: yuschn@163.com
[b]*Hangzhou Tianchuang Environmental Technology Co., Ltd., Hangzhou 311121, China*

Received 21 June 2013; Accepted 16 October 2013

ABSTRACT

Separation efficiency and stability of two lab-fabricated polysulfonamide (PSA) and polypiperazineamide (PA) thin-film composite nanofiltration membranes in long-term filtration of copper sulphate and sulphuric acid mixture were evaluated and compared in this study. The PSA and PA membranes were fabricated through interfacial polymerization process and 60-day long-term filtration tests were carried out with an acidic aqueous solution containing 2.5% (w/v) $CuSO_4$ and 8.0% (w/w) H_2SO_4 under 25.0°C and 10.0 bar. The separation efficiency was studied in terms of permeate flux and retentions to copper and acid. The change of separation efficiency with filtration time was investigated to evaluate the performance stability of the membranes studied. Attenuated total reflectance Fourier transform infrared, field emission scanning electron microscopy, streaming potential analyzer, and contact angle analyzer were also adopted to characterize the change of membrane surface property during filtration. It was found that the PSA membrane maintained its separation efficiency during the 60-day continuous filtration, exhibiting a copper retention of about 83.5% and a sulphuric acid retention of less than 5.0%. The PA membrane began to lose its selectivity after 20 days of filtration due to the deterioration of its skin layer, which was confirmed by the change of membrane surface property.

Keywords: Nanofiltration; Thin-film composite membrane; Copper sulphate and sulphuric acid mixture; Acid stability; Polysulfonamide; Polypiperazineamide

1. Introduction

The separation efficiency of nanofiltration process basically depends on the property of the membrane used and the chemical nature of the solution treated [1]. To uncharged solutes, the separation efficiency of the nanofiltration membrane is mainly determined by the steric effect, while to the charged solutes, it is mainly determined by both of the steric hindrance and the electrostatic membrane–solute interaction [2–4]. The chemical nature of the treated fluid, in particular the nature of the ions, ionic strength, and pH, will affect the membrane surface charge, pore size as well as the characteristics of the solutes presented in the fluid, and thereby the separation efficiency [5–8]. Therefore, the study of the relationships among the

*Corresponding author.

separation efficiency, the property of the membrane used, and the chemical nature of the fluid treated is vital for nanofiltration process [9–11].

Currently, most of the research that has been carried out with NF membranes focused on modeling the mass transfer in NF [12–14], characterization of NF membrane [15], and application of NF membrane in wastewater treatment [16–21]. Comparatively, little work has been done to investigate the separation efficiency and stability of NF membrane under very acidic conditions. Platt et al. [22] studied the stability of membranes NF-45, Desal-5 DK, and BPT-NF-1under extreme acidic conditions. It was found that membrane BPT-NF-1 was more stable than membranes NF-45 and Desal-5 DK in 20.0% (w/w) sulphuric acid at 20.0˚C, and the membrane degradation was due to the acid-catalyzed hydrolysis of the selective skin layer in sulphuric acid. Tanninen et al. [23] investigated the long-term acid resistance and selectivity of membranes NF270, Desal-5 DK, Desal KH, BPT-NF-1, and BPT-NF-2 through cross-flow permeation tests with a feed aqueous solution containing 2.5% (w/v) $CuSO_4$ and 8% (w/w) H_2SO_4 at 40.0˚C. They reported that only membranes Desal KH and BPT-NF-2, which were designed to be acid resistant, maintained separation efficiency over the testing period of two months. Guastalli et al. [24] studied the separation of phosphoric acid from rinsing water coming from the aluminum brightening process through nanofiltration using membranes MPF34, MPF36, Desal-5 DK, and Desal-5 DL. It was found that only membranes MPF34 and Desal-5 DK were effective in separating phosphoric acid from rinsing water. However, their stabilities in long-term filtration were not demonstrated. More recently, Ahmad et al. [25] investigated the acid reclamation and copper recovery using low-pressure polypiperazineamide (PA) nanofiltration membrane. They reported that H^+ was poorly retained and the rejection of copper ion was almost constant within pH 2.0–5.0, and optimum acid reclamation and copper recovery could be achieved at higher volume flux. However, the long-term membrane stability and separation efficiency were not reported.

The primary objective of this study was to evaluate and compare the separation efficiency and stability of polysulfonamide (PSA) (newly developed in our lab [26]) and PA thin-film composite nanofiltration membranes in long-term filtration of copper sulphate and sulphuric acid mixture. The studied PSA and PA thin-film composite nanofiltration membranes were fabricated in our lab through the interfacial polymerization of piperazine (PIP) with naphthalene-1,3,6-trisulfonylchloride (NTSC) and trimesoyl chloride (TMC), respectively. Porous polysulfone membrane with the reinforced nonwoven fabric of polypropylene was adopted as the support membrane to eliminate the influence of the reinforced polysulfone support membrane on the stability of the composite nanofiltration membrane under extreme acidic condition. The 60-day long-term filtration tests were carried out with an aqueous solution containing 2.5% (w/v) $CuSO_4$ and 8.0% (w/w) H_2SO_4, a typical composition of the acidic rinse effluent of copper rod refinery, at 25.0˚C and 10.0 bar. The separation efficiency was studied in terms of permeate flux and retentions to copper and sulphuric acid. The change of separation performance with filtration time was used to investigate the stability of the NF membranes in long-term filtration under acidic condition. Attenuated total reflectance Fourier transform infrared (ATR-FTIR) spectroscopy, field emission scanning electron microscopy (FE-SEM), streaming potential analyzer, and contact angle analyzer were also adopted to characterize the membrane surface property.

2. Experimental setup

2.1. Materials

Polypropylene nonwoven fabric (basic weight = 110 g/m^2, Meida Co. Ltd., China) and polysulfone (Udel P-3500 LCD, Solvay) were used to fabricate the reinforced porous polysulfone support membrane. Monomers such as PIP, TMC, and NTSC were used to form the active layer of the thin-film composite nanofiltration membranes; TMC (purity: 98.0%) and PIP (purity: 99.5%) were purchased from Sigma Aldrich, and NTSC (purity: 98.0%) was synthesized in our laboratory [26]. Isopar G (Isoparaffin type hydrocarbon oil, Guangdong Jesan Chemical Ltd. China) was used to prepare the organic phase solution. Polyethylene glycol (PEG) with molecular weights of 200, 300, 400, 600, 1,000, 1,450, 3,350, 6,000, 10,000, 20,000, 35,000, and 100,000 Da (Sigma-Aldrich) was used as the model solutes to determine the molecular weight cut-off (MWCO) of the membranes prepared. Other chemicals involved were all of analytical grade and used with no further purification.

2.2. Preparation and acid stability evaluation of polysulfone support membrane

Porous polysulfone support membrane was fabricated through phase inversion technique [27,28]. A casting solution containing 13.0% (w/w) polysulfone, 74.5% (w/w) N,N-dimethylacetamide, and 12.5% (w/w) PEG (600 Da) was firstly prepared through

stirring for 10 h at 70.0˚C and degassing for 4.0 h at 50.0˚C. The casting solution was then spread using a knife blade with a 0.28 mm knife gape over a polypropylene nonwoven fabric that was attached to a clean glass plate with laboratory tape. The entire assembly was immediately immersed into a room temperature bath containing de-ionized water. Phase inversion occurred immediately and the solution layer gelled into a white porous sheet. The precipitated reinforced polysulfone membrane was washed thoroughly with de-ionized water and stored wetly.

The acid stability of the fabricated polysulfone support membrane with the reinforced nonwoven fabric of polypropylene was evaluated through acid soaking tests [22]. The acid soaking tests were performed in Pyrex glass bottles covered with polytetrafluoroethylene caps. The fabricated polysulfone support membrane samples were immersed in 8.0% (w/w) H_2SO_4 aqueous solution at 25.0˚C for a period of 60 days. After which, the membrane samples were removed from the acidic solution and rinsed thoroughly with flowing de-ionized water, and then stored in de-ionized water at room temperature until they were characterized for permeation properties.

2.3. Preparation of thin-film composite nanofiltration membrane

Thin-film composite nanofiltration membrane was prepared by coating the surface of the porous polysulfone support membrane with a selective layer through interfacial polymerization technique.

Thin-film composite NF membrane with the selective layer of PSA was fabricated according to the method reported in our previous work [26], with a small modification. PIP and NTSC were used as monomers to form PSA barrier layer with the aid of triethylamine used as a catalyst. First, the polysulfone support membrane was immersed in an aqueous solution of PIP for 2.0 min. Excess solution was drained from the surface of the support membrane using air knife and the amine-saturated support membrane was air dried at room temperature until no liquids remained. Afterwards, the surface of the amine-saturated support membrane was contacted with the organic solution of NTSC for a residence time of 5.0 min. After air drying for 30.0 s, the surface of the membrane was contacted with another organic solution of NTSC for 3.0 min for improving selectivity. Finally, the resulting composite membrane was heat cured at 95.0˚C for 5.0 min, washed thoroughly with de-ionized water, and stored in de-ionized water at 5.0˚C.

Thin-film composite NF membrane with the selective layer of PA was fabricated according to the method reported previously [29]. PIP and TMC were used as monomers to form the PA barrier layer with the aid of triethylamine used as a catalyst. The polysulfone support membrane was immersed in an aqueous solution of PIP for 2.0 min before draining off the excess solution from the soaked surface, and then the amine-saturated support membrane was air-dried at room temperature until no liquids remained. Afterwards, the surface of the amine-saturated support membrane was contacted with the organic solution of TMC for 40.0 s. The membrane was drained and held in a hot air dryer of 70.0˚C for 5.0 min so that a skin layer formed on the support membrane. Finally, the resulting membrane was washed thoroughly with de-ionized water and stored in de-ionized water at 5.0˚C.

2.4. Cross-flow filtration setup and tests

A laboratory-scale filtration setup, as schematically shown in Fig. 1, was employed to carry out the cross-flow filtration tests. The setup mainly contains feed tank, heat exchanger, pump, valves, and two parallel rectangular plate-and-frame filtration cells having an effective membrane area of 19.0 cm^2. All the permeation tests were conducted under constant temperature of 25.0˚C in a total recirculation model, under which both the permeate and concentrate were recycled into the feed tank.

Prior to filtration, membrane coupons loaded in the filtration cells were pressured at 5.0 and 15.0 bar, respectively, with de-ionized water for 2.0 h to ensure stable membrane permeate flux. The pure water fluxes and retentions to PEG (35,000 Da) of the virgin and acid-treated support membranes were determined through permeation tests with de-ionized water and 50 mg/l PEG aqueous solution, respectively, under the pressure of 1.0 bar. The pure water permeability (PWP) of the thin-film composite membrane was determined through permeation tests with de-ionized water under different feed pressures, and the MWCO was determined through permeation tests with aqueous solution containing 50 mg/l PEG with molecular weights of 200, 300, 400, 600, 1,000, 1,450, 3,350, and 6,000 Da, respectively. MWCO was taken as the interpolated value corresponding to 90% from the PEG retention curve [15]. The rejections of the composite membranes to different salts were evaluated through permeation tests with a feed of electrolyte solution containing 500 mg/l salt under the constant pressure of 5.0 bar.

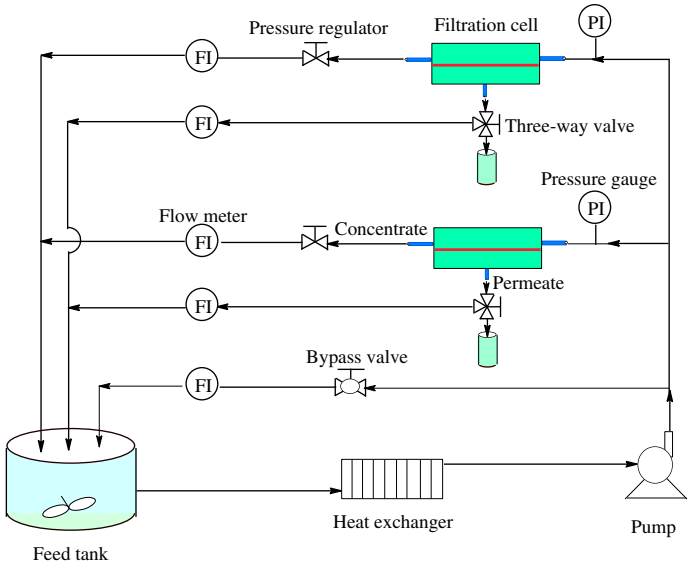

Fig. 1. Schematic diagram of the flat-sheet cross-flow filtration setup.

The 60-day long-term cross-flow filtration tests were then carried out with the composite nanofiltration membranes using a feed aqueous solution containing 2.5% (w/v) $CuSO_4$ and 8.0% (w/w) H_2SO_4 under recirculation mode. The filtration tests were conducted under constant pressure of 10.0 bar, temperature of 25.0°C, cross-flow velocity of 0.5 m/s, and recovery rate of around 4.0%. The separation performance was evaluated in terms of permeate water flux and the retentions of Cu^{2+} and H^+. Measurements of the permeate flux and rejections of Cu^{2+} and H^+ were made at the start, end, and several points during the test.

2.5. Analytical methods

The permeate water flux was determined by measuring the permeate volume collected over a certain period in terms of liter per square meter per hour (l/m^2 h) and calculated using the following equation:

$$J_v = \frac{V}{A \times t} \tag{1}$$

where J_v is the volumetric permeate water flux, A is the effective area of the membrane for permeation, and V is the volume of permeate over a time interval of t.

The observed solute rejection, R, was evaluated using the following equation:

$$R\,(\%) = \frac{C_f - C_p}{C_f} \times 100 \tag{2}$$

where C_P and C_f are the solute concentrations in permeate and feed streams, respectively.

For membrane characterization, the PEG concentrations in feed and permeate were determined using a spectrometric titration at 535 nm after iodine complexation [30], the salt concentrations were obtained through the measurement of the conductivity of the aqueous solution using a conductivity meter (DDSJ-308A, Cany Precision Instruments, China).

For long-term filtration of copper sulphate and sulphuric acid mixture, the concentration of H^+ was measured by titration, the concentration of Cu^{2+} was calculated from the measured concentration of H^+ and the total content of SO_4^{2-}, which was measured by ultraviolet-visible spectrophotometer (UV759, Shanghai) at 470 nm after precipitation with Ba^{2+} [26].

ATR-FTIR Spectroscopy (Nicolet Avatar 370 FTIR spectrometer with a ZnSe crystal as the internal refection element with an angle of incidence of 45°) was adopted to determine the surface chemistry of the membrane. FE-SEM (Hitachi S-4800, Japan) was employed to characterize the surface and cross-section structures of the composite. DSA10-MK2 contact angle analyzer (KRUSS BmbH, Germany) was employed to measure the surface water contact angle through sessile drop method at 25.0°C. Images were captured 5 s

after introducing the drop and the contact angles were calculated. At least 10 measurements on different locations of the membrane sample with the size of 0.5 cm × 5.0 cm were performed and averaged. Anton Paar zeta potential analysis meter (Austria) was employed to conduct the measurement of the streaming potential of the membrane surface, which was carried out with 0.001 mol/l KCl aqueous solution at 25 ± 1.0°C and pH ranging from 1.5 to 9.0. Surface zeta potentials were determined from the measured streaming potentials according to the Helmholtz–Smoluchowski equation with the Fairbrother and Mastin substitution [31]. The data presented were average values from three samples of each membrane type. All the membrane samples for ATR-FTIR, FE-SEM and contact angle measurement were dried at 25.0°C under vacuum for at least 10.0 h.

3. Results and discussion

3.1. Permeation properties of the virgin and acid-soaked polysulfone support membranes

The permeation properties of the virgin and acid-soaked lab-fabricated porous polysulfone support membranes were characterized in terms of PWP and retention to PEG with the molecular weight of 35,000 Da. The PWP was determined through the measurement of pure water flux under the applied pressure of 1.0 bar. The results presented in Fig. 2 clearly illustrate that the polysulfone support membrane used in this study maintains its permeation properties after soaking in 8.0% (w/v) H_2SO_4 aqueous solution at 25.0°C for 60 days and exhibits good acid stability. The PWP and the retention to PEG with the molecular weight of 35,000 Da are about 190 l/m^2 h bar and 83.5%, respectively.

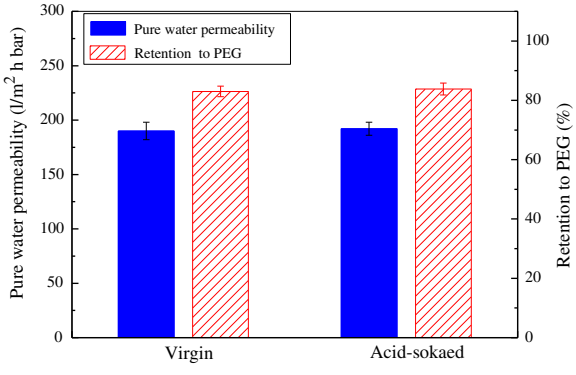

Fig. 2. PWP ( ) and retention to PEG with molecular weight of 35,000 Da ( ) for the virgin and acid-soaked polysulfone support membranes determined with de-ionized water and 50 mg/l PEG aqueous solution, respectively, at 1.0 bar, 25°C and pH 7.0.

3.2. Properties of the studied PSA and PA thin-film composite NF membranes

Thin-film composite membranes with the active skin layers of PSA and PA on the reinforced porous polysulfone support membrane were prepared by *in situ* interfacial polymerization of PIP in water with NTSC and TMC in organic solvent, respectively. The chemical structures of the monomers used and the expected active skin layers of the formed thin-film composite membranes are shown schematically in Fig. 3. The properties of the lab-fabricated PSA and PA thin-film composite membranes were characterized in terms of PWP, rejections to different salts, MWCO, surface zeta potential, and surface hydrophilicity.

The PWP was determined by measuring the de-ionized water fluxes at different operating pressures. As shown in Fig. 4, the pure water fluxes of the two studied NF membranes increase linearly with increasing applied pressure in accordance to the Spiegler–Kedem equation [32], and the PWP is about 4.2 and 5.8 l/m^2 h bar for the prepared PSA and PA membranes, respectively.

The salt rejection characteristics of the prepared NF membranes were studied in terms of five different salts of $MgCl_2$, NaCl, $CuSO_4$, $MgSO_4$, and Na_2SO_4 through cross-flow permeation tests conducted at feed salt concentration of 500 mg/l, pressure of 5.0 bar, and pH of 6.8. As shown in Fig. 5, under the testing pH of 6.8, the rejections of the studied NF membranes to different salts follow the same order of $MgCl_2 < NaCl < CuSO_4 < MgSO_4 < Na_2SO_4$, which is a typical characteristic of negatively charged polymeric nanofiltration membranes [33].

The MWCO of the fabricated membrane was determined through permeation tests using a group of PEG with molecular weights of 200, 300, 400, 600, 1,000, 1,450, 3,350, and 6,000 Da as model solutes. The retentions to different PEG fractions are presented in Fig. 6, from which we can find that the MWCO is about 2,200 and 380 Da for the PSA and PA membranes, respectively.

The surface zeta potentials of the prepared thin-film composite membranes were studied through streaming potential measurements. The measured zeta potentials of the composite membranes under different pHs are presented in Fig. 7, from which one can see that both the lab-fabricated PSA and PA membranes have amphoteric surface with an isoelectric point of about pH 2.6 and 3.0, respectively. At acidic pH of

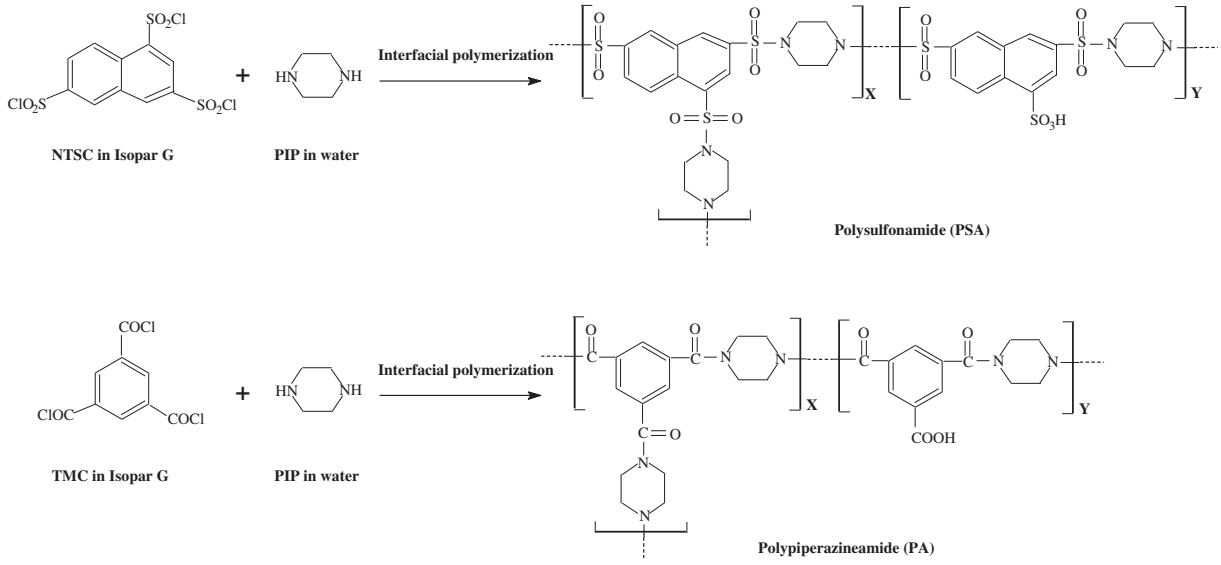

Fig. 3. Structures of the PSA and PA skin layers formed by interfacial polymerization of PIP with NTSC and TMC, respectively.

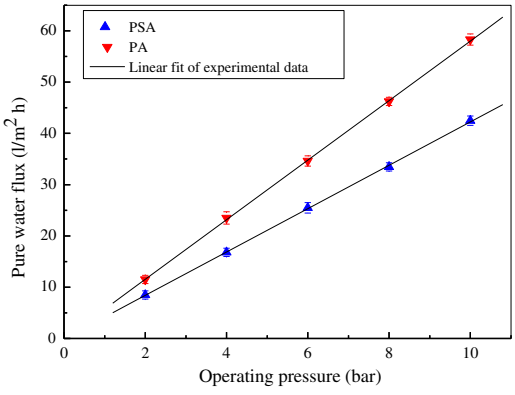

Fig. 4. Pure water flux as a function of operating pressure for the lab-fabricated PSA (▲) and PA (▼) membranes tested with de-ionized water at 25.0℃.

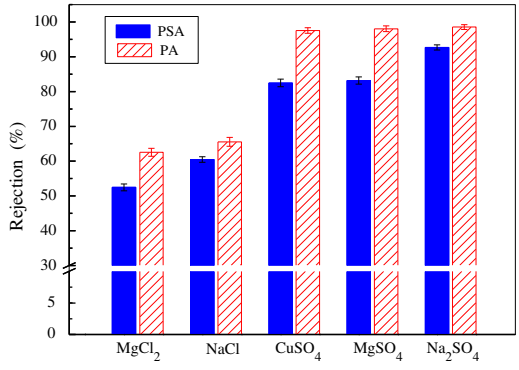

Fig. 5. Rejections for the lab-fabricated PSA ( ) and PA ( ) membranes tested with 500 mg/l electrolyte solution at 5.0 bar, 25.0℃, and pH 6.8.

less than 2.0, the surface of PSA membrane is more positively charged than that of PA membrane.

3.3. *Performance of the NF membranes in long-term filtration of copper/acid mixture*

The 60-day long-term continuous filtration tests were carried out with a feed aqueous solution containing 8.0% (w/w) sulphuric acid and 2.5% (w/v) copper sulphate under the constant temperature of 25℃ and pressure of 10.0 bar employing the two lab-fabricated NF membranes. Under this very acidic condition, the surfaces of the two lab-fabricated membranes are positively charged, the positive surface charge rejects cations, sulphuric acid will permeate quite freely across the membrane [34], while the metal ion Cu^{2+} will be retained by the membrane due to the Donnan exclusion between the Cu^{2+} and the positively charged membrane surface [35]. Therefore, the separation of H_2SO_4 from copper sulphate can be achieved.

The fluxes of the two studied nanofiltration membranes during the 60-day continuous filtration are presented in Fig. 8. It can be seen from the figure that the lab-fabricated thin-film composite nanofiltration membrane with the selection layer of PA exhibits a relatively higher flux than the membrane with the selection layer of PSA during the whole period of

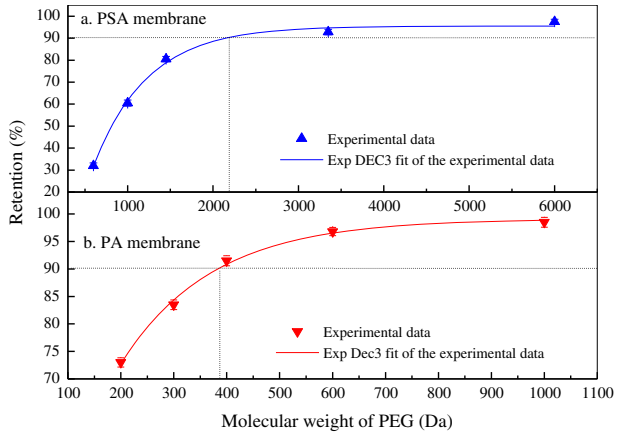

Fig. 6. PEG retention curves for the lab-fabricated PSA (▲) and PA (▼) membranes tested with 50 mg/l PEG aqueous solution at 5.0 bar, 25℃, and pH 7.0.

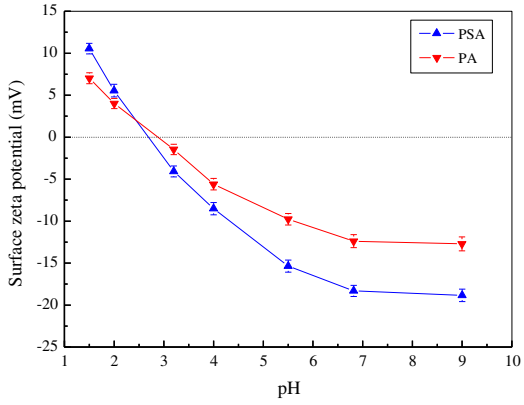

Fig. 7. Surface zeta potential as a function of pH for the lab-fabricated PSA (▲) and PA (▼) NF membranes tested with 0.001 mol/l KCl aqueous solution at 25.0℃.

filtration. The PSA membrane shows little variation in permeate flux during the whole period of filtration, exhibiting a measured steady flux of about 19.0 l/m^2 h at 10.0 bar and 25℃, while significant change in permeate flux is observed with the PA composite membrane. The slight augment of the permeate flux of the PA membrane at the first 10-day filtration is ascribed to the partial hydrolysis of the amide bonds, which results in a more hydrophilic and permeable skin layer. The significant increase in the flux of the PA membrane after 30 days of filtration indicates deterioration of the selective surface layer. The difference in the change of flux with filtration time suggests that the PSA NF membrane possesses better acid stability than PA NF membrane in long-term filtration under extreme acidic condition. The measured steady flux of the studied PSA membrane is relatively higher than

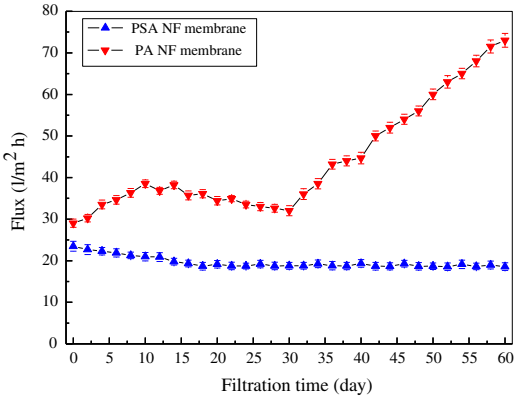

Fig. 8. Changes of fluxes with filtration time for the lab-fabricated PSA (▲) and PA (▼) NF membranes in long-term filtration of aqueous solution containing 8.0% (w/w) H_2SO_4 and 2.5% (w/v) $CuSO_4$ at 10.0 bar and 25.0℃.

the reported steady flux (about 20 l/m^2 h at 30 bar and 40℃) of the commercial acid stable NF membrane Desal KH in filtration aqueous solution containing 8.0% (w/w) sulfuric acid and 2.5% (w/v) copper sulphate [23].

The changes of copper retentions of the two lab-fabricated NF membranes during the 60-day filtration are demonstrated in Fig. 9. What is apparent from the graph is that, as the filtration time prolongs, the PSA composite membrane maintains its selectivity and exhibits an overall observed copper retention of around 83.5% at 10 bar, while the PA composite membrane shows excellent copper retention of higher than 98.0% during the first 20-day operation, and then starts to lose its selectivity and exhibits a much poor

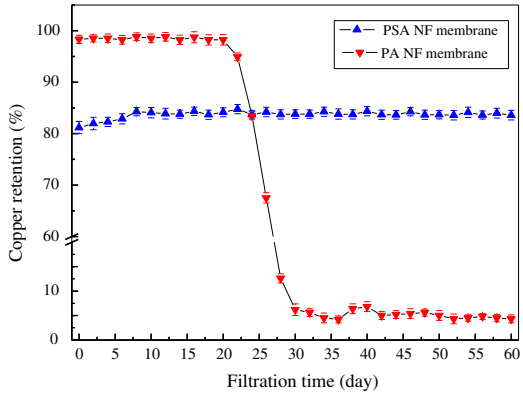

Fig. 9. Changes of copper retentions with filtration time for the lab-fabricated PSA (▲) and PA (▼) NF membranes in long-term filtration of aqueous solution containing 8.0% (w/w) H_2SO_4 and 2.5% (w/v) $CuSO_4$ at 10.0 bar and 25.0℃.

copper retention of less than 5.0% after 30 days of filtration at 25.0˚C. The higher copper retention of the PA membrane during the first 20-day filtration is attributed to its relatively small pore size compared to the studied PSA membrane, while the loss of selectivity of the PA membrane is due to the hydrolysis and deterioration of the PA skin layer under acidic condition. The minor change of copper retention with filtration time also demonstrates that the studied PSA NF membrane possesses excellent acid stability in long-term filtration under very acidic condition. The lab-fabricated PSA membrane can be applied in the treatment of acidic rinse waters (containing sulphuric acid) of copper rod refinery and other acidic effluents from metal industrials. However, it should be mentioned here that the steady copper retention of the studied PSA NF membrane was relatively lower than that of the commercial acid stable nanofiltration membrane Desal KH, which exhibited an overall copper retention of 92–95% during a 60-day filtration of aqueous solution containing 8.0% (w/w) sulfuric acid and 2.5% (w/v) copper sulphate at 30.0 bar and 40˚C [23]. Therefore, the separation efficiency of the acid stable PSA nanofiltration membrane developed in our lab needs to be further improved.

Fig. 10 presents the changes of the calculated sulphuric acid retentions of the two studied NF membranes during the 60-day continuous filtration. It is illustrated that the changes of acid retention with filtration time for the studied PSA and PA NF membranes are much different. Deterioration can be further observed from the acid retention curve of PA NF membranes, the sulphuric acid retention for the PA NF membrane declines slowly from about 26.0 to 22.0% during the first 20-day operation and then decreases dramatically to a much lower value of about 6.0% after 30 days of filtration. On the other hand, for the PSA NF membrane developed in our lab, the sulphuric acid permeates quite freely and the acid retention is always less than 5.0% over the whole filtration period.

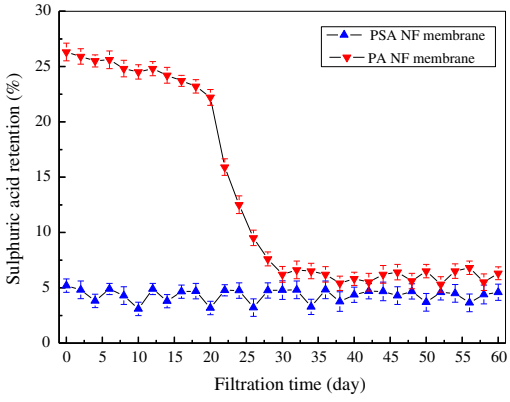

Fig. 10. Changes of sulfuric acid retentions with running time for the lab-fabricated PSA (▲) and PA (▼) membranes in long-term filtration of aqueous solution containing 8.0% (w/w) H_2SO_4 and 2.5% (w/v) $CuSO_4$ at 10.0 bar and 25.0˚C.

3.4. Changes of surface properties of the NF membranes in long-term filtration of copper/acid mixture

It is known from literature that the structural and morphological changes taking place in the active layer of composite NF membranes as a result of acid degradation could be revealed through complementary characterization techniques [36]. Therefore, the changes in the membrane surface property of the studied NF membranes during the long-term filtration of copper/acid mixture were further studied to figure out the change of the separation performance of the studied NF membrane.

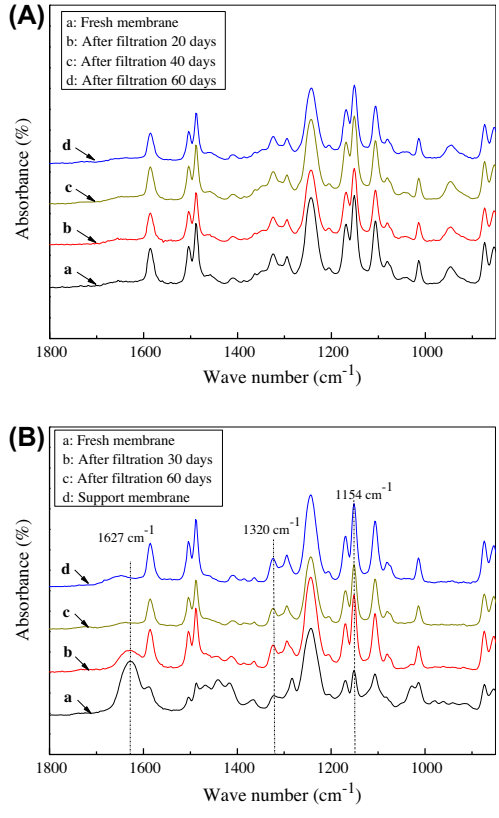

Fig. 11. ATR-FTIR spectra for the lab-fabricated PSA (A) and PA (B) NF membranes before and after filtration with copper/acid mixture for a certain period.

Surface chemical structure was characterized by using ATR-FTIR. The infrared spectra of the fresh and used membranes, recorded as a function of increasing filtration time, are displayed in Fig. 11, which also shows the ATR-FTIR spectrum of the porous polysulfone support membrane. The consistency of the ATR-FTIR spectra of the PSA NF membrane before and after filtration (Fig. 11(A)) indicates that no chemical change has occurred with the PSA skin layer during the whole filtration. While for the PA NF membrane (Fig. 11(B)), as the filtration time prolongs, the intensity of the characteristic peak of amide (–CONH–) at around 1,627 cm^{-1} decreases gradually, indicating the hydrolysis of the amide bonds of the PA skin layer, and the intensities of the characteristic peaks of polysulfone support membrane at about 1,320 and 1,154 cm^{-1} increase continuously, revealing the exposure of the polysulfone support membrane resulting from the fully hydrolysis of the PA skin layer. The results of ATR-FTIR analysis confirm that the PSA NF membrane possesses better acid stability than PA NF membrane in long-term filtration under extreme acidic condition.

Surface morphological structure was investigated by using FE-SEM. The FE-SEM images of the surfaces of the fresh and used membranes are presented in Fig. 12. Many pinholes and cracks are observed on the surface of the used PA NF membrane (Fig. 12(b)), indicating the occurrence of degradation of the selective layer of the studied PA NF membrane during filtration. On the other hand, no obvious change is observed with the surface of the used PSA NF membrane (Fig. 12(d)) and the morphological structure of the surface layer of the studied PSA membrane is relatively stable under extreme acidic condition. Additionally, the thickness of the skin layer of the used PSA membrane (Fig. 12(e)) is more uniform and thicker than that of the used PA membrane (Fig. 12(f)). The degradation of PA membrane is mainly due to the acid-catalyzed hydrolysis of the PA skin layer in sulfuric acid aqueous solution [37].

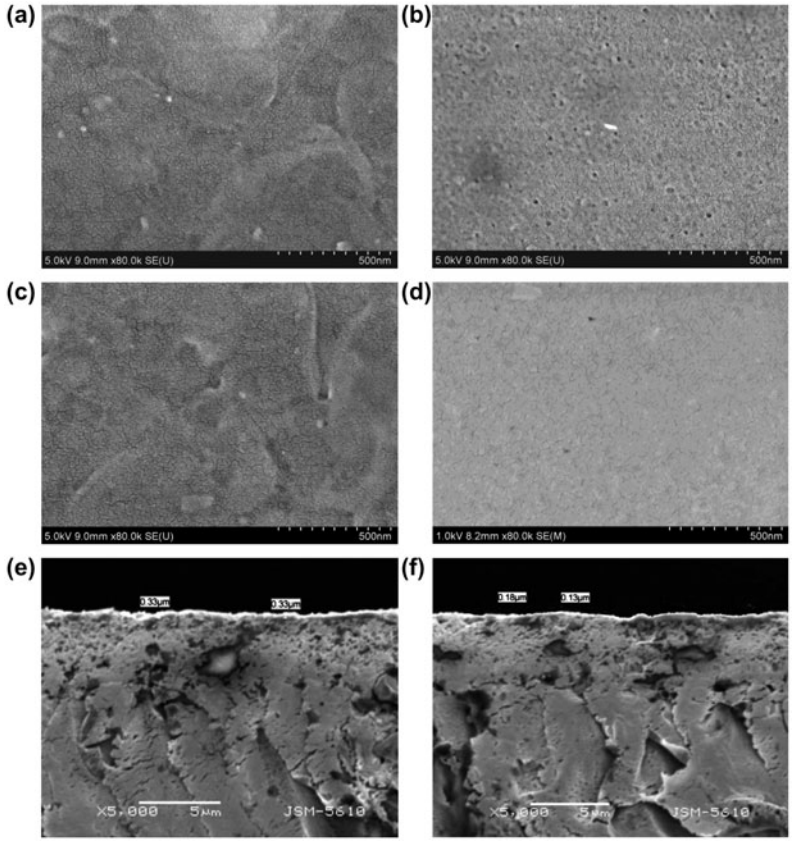

Fig. 12. FE-SEM images of (a) surface of fresh PA membrane, (b) surface of used PA membrane, (c) surface of fresh PSA membrane, (d) surface of used PSA membrane, (e) cross-section of used PSA membrane, and (f) cross-section of used PA membrane.

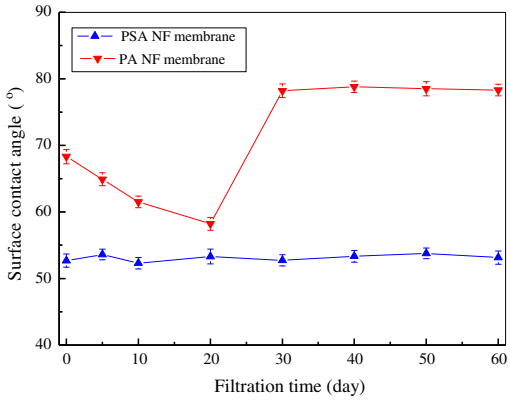

Fig. 13. Changes of surface contact angle with filtration time for the lab-fabricated PSA (▲) and PA (▼) NF membranes.

Hydrolysis of the active skin layer of the polyamide thin-film composite membrane always generates a lot of hydrophilic groups, and thereby changing the surface hydrophilicity of the composite membrane [36]. Thus, the stability of the studied NF membrane was also studied in terms of the change of membrane surface hydrophilicity, which is evaluated through the measurement of contact angle between the membrane surface and the air-water interface. The measured surface contact angles of the fresh and used membranes, recorded as a function of increasing filtration time, are presented in Fig. 13. The minor variation in the surface contact angle with filtration time indicates that no hydrolysis is occurred with the PSA active layer during the whole filtration period, while the significant change in surface contact angle demonstrates the occurrence of hydrolysis of the PA skin layer. The decrease of the measured surface contact angle of the PA NF membrane from about 68.0° to 58.0° at the initial stage is ascribed to the partial hydrolysis of amide bonds, while the significant increase of the measured surface contact angle from about 58.0° to 78.0°, as the filtration time prolongs from 20 to 30 days, is attributed to the exposure of polysulfone support membrane as the result of the complete deterioration of skin PA layer under acidic condition.

4. Conclusions

In this work, the separation efficiency and stability of the lab-fabricated PSA and PA thin-film composite nanofiltration membranes in long-term filtration of sulphuric acid and copper sulphate mixture were investigated. The following conclusions can be drawn from the experimental results:

(1) In 60-day long-term continuous filtration of aqueous solution containing 2.5% (w/v) $CuSO_4$ and 8.0% (w/w) H_2SO_4 under 10.0 bar and 25.0°C, the PSA NF membrane showed excellent performance stability and exhibited a stable copper retention of about 83.5%, a steady flux of around 19.0 l/m^2 h and a relatively low sulphuric acid retention of less than 5.0%, while the PA NF membrane only maintained its good separation efficiency at the beginning of the filtration and began to lose its selectivity after 20 days of filtration due to the deterioration of the polyamide skin layer. The PSA nanofiltration membrane possessed better overall selectivity (separation of H_2SO_4 from copper sulphate) under extreme acidic conditions and was suitable for the treatment of acidic effluents from metal industrials.

(2) The results of surface chemical structure analysis by ATR-FTIR revealed that no evident chemical change occurred with the skin layer of the used PSA membrane, but hydrolysis and exposure of polysulfone support membrane occurred with the used PA membrane. Unlike the PSA NF membrane, the emergence of pinholes and cracks on the surface of the used PA NF membrane also indicated the deterioration of the skin layer of PA membrane during the long-term filtration. Furthermore, the stability of PSA skin layer was demonstrated by the minor variation in the surface contact angle, while the hydrolysis of the PA surface skin layer followed by the exposure of polysulfone support membrane was confirmed by the significant change of the measured surface contact angle.

Acknowledgments

The authors gratefully acknowledge the financial support of the National Nature Science Foundation of China (NNSFC) (Grant No. 21276242), the National High-tech R&D Program of China (863 Program) (No. 2012AA03A601) and the Zhejiang Provincial Key Innovation Team (No. 2010R50038).

References

[1] A.I. Schafer, A.G. Fane, T.D. Waite, Nanofiltration—Principles and Applications, Elsevier Advanced Technology, Oxford, 2005.
[2] M. Mulder, Basic Principles of Membrane Technology, 2nd ed., Kluwer Academic Publishers, Boston, 1996.
[3] B. Van der Bruggen, J. Schaep, D. Wilms, C. Vandecasteele, Influence of molecular size, polarity and charge on the retention of organic molecules by nanofiltration, J. Membr. Sci. 156 (1999) 29–41.

[4] N.S. Kotrappanavar, A.A. Hussain, M.E.E. Abashar, I.S. Al-Mutazc, T.M. Aminabhavi, M.N. Nadagouda, Prediction of physical properties of nanofiltration membranes for neutral and charged solutes, Desalination 280 (2011) 174–182.
[5] M.R. Teixeira, M.J. Rosa, M. Nystrom, The role of membrane charge on nanofiltration performance, J. Membr. Sci. 265 (2005) 160–166.
[6] L. Braeken, B. Bettens, K. Boussu, P. Van der Meeren, J. Cocquyt, J. Vermant, B. Van der Bruggen, Transport mechanisms of dissolved organic compounds in aqueous solution during nanofiltration, J. Membr. Sci. 279 (2006) 311–319.
[7] P. Dey, L. Linnanen, P. Pal, Separation of lactic acid from fermentation broth by cross flow nanofiltration: Membrane characterization and transport modeling, Desalination 288 (2012) 47–57.
[8] F. Fadaei, V. Hoshyargar, S. Shirazian, S.N. Ashrafizadeh, Mass transfer simulation of ion separation by nanofiltration considering electrical and dielectrical effects, Desalination 284 (2012) 316–323.
[9] S. Gomes, S.A. Cavaco, M.J. Quina, L.M. Gando-Ferreira, Nanofiltration process for separating Cr(III) from acid solutions: Experimental and modeling analysis, Desalination 254 (2010) 80–89.
[10] B. Eren, R. Ileri, E. Dogan, I. Koyuncu, Development of artificial neural network for prediction of salt recovery by nanofiltration from textile industry wastewaters, Desalin. Water Treat. 50 (2012) 317–328.
[11] G. Ribera, L. Llenas, M. Rovira, J. de Pablo, X. Martinez-Llado, Pilot plant comparison study of two commercial nanofiltration membranes in a drinking water treatment plant, Desalin. Water Treat. 51(1–3) (2013) 448–457.
[12] S. Darvishmanesh, A. Buekenhoudt, J. Degrève, B. Van der Bruggen, Coupled series–parallel resistance model for transport of solvent through inorganic nanofiltration membranes, Sep. Purif. Technol. 70 (2009) 46–52.
[13] H. Kelewou, A. Lhassani, M. Merzouki, P. Drogui, B. Sellamuthu, Salts retention by nanofiltration membranes: Physicochemical and hydrodynamic approaches and modeling, Desalination 277 (2011) 106–112.
[14] R. Wang, Y. Li, J. Wang, G. You, C. Cai, B.H. Chen, Modeling the permeate flux and rejection of nanofiltration membrane separation with high concentration uncharged aqueous solutions, Desalination 299 (2012) 44–49.
[15] N. Hilal, M. Al-Abria, H. Al-Hinaib, M. Abu-Arabic, Characterization and retention of NF membranes using PEG, HS and polyelectrolytes, Desalination 221 (2008) 284–293.
[16] A. Bes-Piá, B. Cuartas-Uribe, J.-A. Mendoza-Roca, M.I. Alcaina-Miranda, Study of the behaviour of different NF membranes for the reclamation of a secondary textile effluent in rinsing processes, J. Hazard. Mater. 178 (2010) 341–348.
[17] M.J. Lopez-Munoz, A. Sotto, J.M. Arsuaga, Nanofiltration removal of pharmaceutically active compounds, Desalin. Water Treat. 42 (2012) 138–143.
[18] M. Jacob, C. Li, C. Guigui, C. Cabassud, G. Lavison, L. Moulin, Performance of NF/RO process for indirect potable reuse: Interactions between micropollutants, micro-organisms and real MBR permeate, Desalin. Water Treat. 46 (2012) 75–86.
[19] C.S. Ong, W.J. Lau, A.F. Ismail, Treatment of dyeing solution by NF membrane for decolorization and salt reduction, Desalin. Water Treat. 50 (2012) 245–253.
[20] D. Wu, W. Wang, S. Chen, Z. Yang, G. Tian, S. Ali Baig, Q. Mahmood, Advanced bamboo industry wastewater treatment through nanofiltration membrane technology, Desalin. Water Treat. 51(16–18) (2013) 3454–3462.
[21] D. Dolar, M. Perisa, K. Kosutic, S. Babic, NF/RO removal of enrofloxacin and its photodegradation products from water, Desalin. Water Treat. 51(1–3) (2013) 469–475.
[22] S. Platt, M. Nyström, A. Bottino, G. Capannelli, Stability of NF membranes under extreme acidic conditions, J. Membr. Sci. 239 (2004) 91–103.
[23] J. Tanninen, S. Platt, A. Weis, M. Nyström, Long-term acid resistance and selectivity of NF membranes in very acidic conditions, J. Membr. Sci. 240 (2004) 11–18.
[24] A.R. Guastalli, J. Labanda, J. Llorens, Separation of phosphoric acid from an industrial rinsing water by means of nanofiltration, Desalination 243 (2009) 218–228.
[25] A.L. Ahmad, B.S. Ooi, A study on acid reclamation and copper recovery using low pressure nanofiltration membrane, Chem. Eng. J. 156 (2010) 257–263.
[26] M. Liu, G. Yao, Q. Cheng, M. Ma, S. Yu, C. Gao, Acid stable thin-film composite membrane for nanofiltration prepared from naphthalene-1,3,6-trisulfonylchloride (NTSC) and piperazine (PIP), J. Membr. Sci. 415–416 (2012) 122–131.
[27] B. Chakrabarty, A.K. Ghoshal, M.K. Purkait, Preparation, characterization and performance studies of polysulfone membranes using PVP as an additive, J. Membr. Sci. 315 (2008) 36–47.
[28] M.K. Sinha, M.K. Purkait, Increase in hydrophilicity of polysulfone membrane using polyethylene glycol methyl ether, J. Membr. Sci. 437 (2013) 7–16.
[29] M. Liu, S. Yu, Y. Zhou, C. Gao, Study on the thin-film composite nanofiltration membrane for the removal of sulfate from concentrated salt aqueous: Preparation and performance, J. Membr. Sci. 310 (2008) 289–295.
[30] A.D. Sabde, M.K. Trivedi, V. Ramachandhran, M.S. Hanra, B.M. Misra, Casting and characterization of cellulose acetate butyrate based UF membranes, Desalination 114 (1997) 223–232.
[31] A.E. Childress, M. Elimelech, Effect of solution chemistry on the surface charge of polymeric reverse osmosis and nanofiltration membranes, J. Membr. Sci. 119 (1996) 253–268.
[32] K.S. Spiegler, O. Kedem, Thermodynamics of hyperfiltration (reverse osmosis): Criteria for efficient membranes, Desalination 1 (1966) 311–326.
[33] J.M.M. Peeters, J.P. Boom, M.H.V. Mulder, H. Strathmann, Retention measurements of nanofiltration membranes with electrolyte solutions, J. Membr. Sci. 145 (1998) 199–209.
[34] T.J.K. Visser, S.J. Modise, H.M. Krieg, K. Keizer, The removal of acid sulphate pollution by nanofiltration, Desalination 140 (2001) 79–86.

[35] J. Tanninen, M. Mänttäri, M. Nyström, Nanofiltration of concentrated acidic copper sulphate solutions, Desalination 189 (2006) 92–96.
[36] V. Freger, A. Bottino, G. Capannelli, M. Perry, V. Gitis, S. Belfer, Characterization of novel acid-stable NF membranes before and after exposure to acid using ATR-FTIR, TEM and AFM, J. Membr. Sci. 256 (2005) 134–142.
[37] J. Tanninen, M. Nyström, Separation of ions in acidic conditions using NF, Desalination 147 (2002) 295–299.